

## Nanometric-size effect upon diffusion and reaction in semiconductors: experimental and theoretical investigations

A. Portavoce<sup>1,a</sup>, C. Girardeaux<sup>2,b</sup>, G. Trégli<sup>3,c</sup>, J. Bernardini<sup>1,d</sup>,  
D. Mangelinck<sup>1,e</sup> and L. Chow<sup>4,f</sup>

<sup>1</sup>CNRS, IM2NP, Faculté des Sciences et Techniques de Saint-Jérôme, Case 142, 13397 Marseille, France

<sup>2</sup>Aix-Marseille Université, IM2NP, Faculté des Sciences et Techniques de Saint-Jérôme, Case 142, 13397 Marseille, France

<sup>3</sup>CNRS, CINAM, Campus de Luminy Case 913, 13288 Marseille, France

<sup>4</sup>Department of Physics, University of Central Florida, Orlando, Florida 32816, USA

<sup>a</sup>alain.portavoce@im2np.fr, <sup>b</sup>christophe.girardeaux@im2np.fr, <sup>c</sup>treglia@cinam.univ-mrs.fr,

<sup>d</sup>jean.bernardini@im2np.fr, <sup>e</sup>dominique.mangelinck@im2np.fr, <sup>f</sup>Lee.Chow@ucf.edu

**Keywords:** Diffusion, Reactive Diffusion, size effect, Nanometric Scale, Silicon, Simulation.

**Abstract.** The use of nanometric size materials as embedded clusters, nanometric films, nanocrystalline layers and nanostructures is steadily increasing in industrial processes aiming to produce materials and devices. This is especially true in today Si-based microelectronics with transistors made of a multitude of different thin film materials (B-, As-, and P-doped Si, NiSi(Pt), poly-Si, W, TiO<sub>x</sub>, LaO, SiO<sub>2</sub>, Al, H<sub>2</sub>O<sub>2</sub>...), and exhibiting a characteristic lateral size of 32-22 nm. Size reduction leads to an increasing role of surfaces and interfaces, as well as stress and nano-scale effects upon important phenomena driving fabrication processes, such as atomic diffusion, phase nucleation, phase growth, and coarsening. Consequently, nanotechnology related to Material Science requires an investigation at the nanometric (or atomic) scale of elementary physical phenomena that are well-known at the microscopic scale. This paper is focused on nano-size effects upon diffusion in Si and Si reactive diffusion. We present recent results showing that the kinetic of lattice diffusion is enhanced in semiconductor nanometric (nano-) grains, while grain boundary (GB) diffusion is not changed in nano-GBs. It is also shown that diffusion in triple-junction (TJ) is several orders of magnitude faster than GB diffusion, and that its effect cannot be neglected in nanocrystalline (nc) layers made of 40 nm-wide grains. Experimental results concerning Si sub-nanometric film reaction on Ni(111) substrate are also presented and compared to theoretical results giving new prospects concerning nano-size effects on reactive diffusion at the atomic scale.

### Introduction

Inorganic material nanotechnology involves the use of nano-objects as nano-clusters [1], nanowires [2], and nano-islands [3], or nano-phases as nanometer-thick films and nanocrystalline layers [4], to produce devices or materials exhibiting remarkable electrical, magnetic, mechanical... properties. In the case of microelectronic devices, today's transistors are made of nanometer-thick layers of a large number of different materials (fig. 1). For example, on top of the doped Si channel the high-k dielectric can be made of a stack of Al, HfO<sub>2</sub>, La... covered by a nc-layer playing the role of a metallic gate (TiN). On top of that, a doped polycrystalline Si layer covered by a silicide layer (NiSi(Pt)) in contact with the first metal level (W) is usually found. Furthermore, the transistor's source and drain can contain two or three different dopants and are covered by a thin polycrystalline silicide layer in contact with a polycrystalline metal. In addition, a low-k dielectric (SiO<sub>x</sub>F<sub>y</sub>) is used to separate the different structures and the different metal levels (at least 10 levels: W, Cu, and Al) and several types of nano-layers are used as diffusion barriers (TiN, Ta...). For several decades, the lateral size of the microelectronic devices has been constantly reduced to reach in today Si technology 65 to 22 nm. For different applications, nanotechnology leads to a decrease of the phase

volume sizes and to an increase of the interface number. This may result in significant changes in fabrication processes partly due to the modification of atom transport and phase transformation. In the case of atomic transport, it is necessary to know diffusion coefficients in nano-volumes and at the interfaces, taking into account phenomena such as segregation. For reactive diffusion, the size-effect and the influence of interfaces upon nucleation and reaction kinetics need to be investigated.

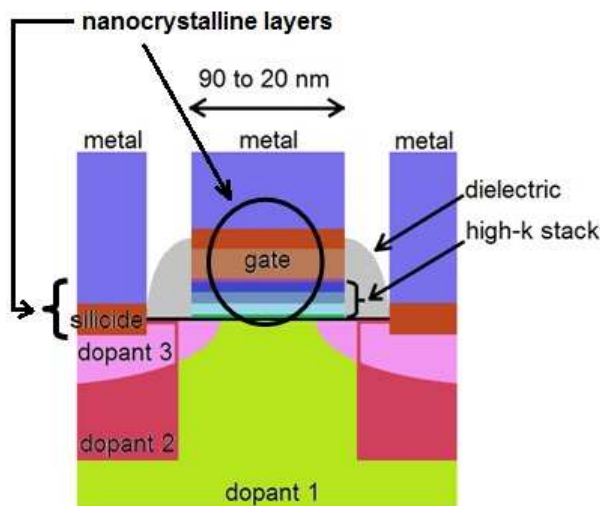


Fig. 1. Transistor schematic.

In order to perform fundamental studies, it is important to be able to control certain parameters such as size, stress etc. in experiments. For example, pure nanocrystalline (nc) materials are interesting to characterize nano-size effects upon diffusion. In this type of sample, atomic diffusion can be studied in a single phase, in a tridimensional (3D) nano-volume (grains), in 2D interfaces (grain boundaries – GBs), and in the 1D defect called triple junctions (TJs). The reaction of a pure single ultra-thin film with a substrate constitutes the simplest case of reactive diffusion. However, even in that case, the phase transformation can be complicated by the formation of a nc-layer following after nucleation, both lateral and normal growth, preventing a simple 1D study. In this paper we present experimental results concerning Ge diffusion in nc-Si [5-6], as well as the comparison between kinetic Monte Carlo (KMC) simulations [7] and experiments [8] related to the reaction of a Si sub-nanometric layer on a Ni(111) substrate.

### Nano-size effect upon atomic diffusion

Fig. 2 presents the Ge GB diffusion coefficients that have been measured in polycrystalline Si exhibiting micrometric grains (mc-Si) [5]. The sample was made from cast silicon used for the growth of Czochralski (or floating-zone) single crystals, exhibiting grains with an average size of  $\sim 30 \mu\text{m}$ . Ge diffusion was measured via standard procedures during type B diffusion kinetic [5].  $^{68}\text{Ge}$  radiotracer was deposited on the sample surface before annealing under pure Ar atmosphere. The Fisher solution was used to extract the GB diffusion coefficients  $D_{\text{gb}}$  from the slope of the Ge penetration profiles, using the Ge lattice diffusion coefficient  $D_{\text{v}}$  measured in monocrystalline Si (mono-Si) either by Hettich et al. [9] or Dorner et al. [10]. However,  $D_{\text{v}}$  from Hettich et al. better corresponds to our experimental temperature range. We found  $D_{\text{gb}} = 316.5 \exp(-3.34 \text{ eV}/kT) \text{ cm}^2 \text{ s}^{-1}$  with  $D_{\text{v}}$  from Hettich et al. and  $D_{\text{gb}} = 19.10 \times 10^4 \exp(-4.05 \text{ eV}/kT) \text{ cm}^2 \text{ s}^{-1}$  with  $D_{\text{v}}$  from Dorner et al., considering that the GB width  $\delta = 0.5 \text{ nm}$ . In order to study Ge diffusion in nc-Si, a Ge dose of  $4.2 \times 10^{14} \text{ cm}^{-2}$  was implanted at 180 keV in a nc-Si layer grown by chemical vapor deposition on a clean Si(001) substrate. The average grain size ( $\sim 40 \text{ nm}$ ) of the nc-Si layer was shown by X-ray diffraction to be the same before and after annealing. Annealing was performed under pure Ar gas flow, and Ge diffusion profiles were measured by secondary ion mass spectrometry (SIMS) [5].

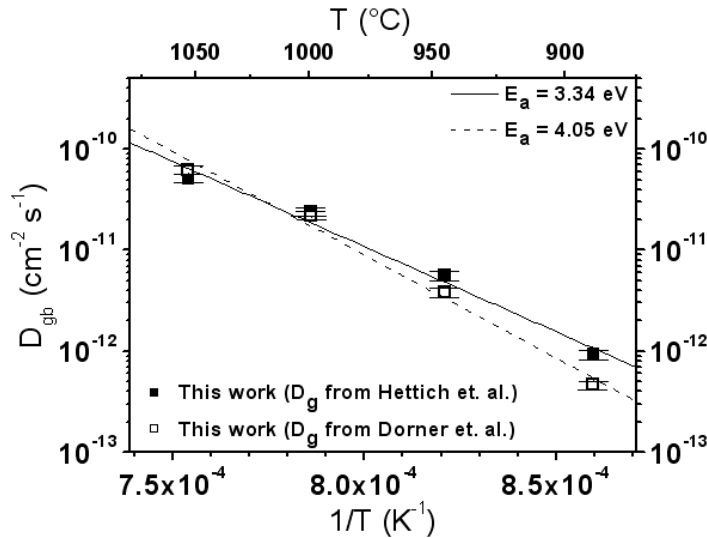


Fig. 2. Ge GB diffusion coefficients measured in a mc-Si layer made of 30  $\mu\text{m}$ -wide grains, using the Fisher model and the Ge lattice diffusion coefficient from either Hettich et al. (solid squares) or Dorner et al. (open squares).

Finite element simulations (FES) were used to measure both  $D_v$  and  $D_{gb}$  in nc-Si, considering either a model with the usual 2D Fisher geometry [5] or a model with a 3D geometry [6]. In contrast with the 2D model, the 3D model allows TJ diffusion, in addition to lattice and GB diffusion, to be considered. Fig. 3 presents the comparison between Ge diffusion coefficients found in mc-Si (broken lines) and nc-Si (open circles for the 2D geometry and solid circles for the 3D geometry). Simulations with the 3D geometry were performed considering a constant TJ diffusion coefficient  $D_{Tj} = 10^{-9} \text{ cm}^2 \text{ s}^{-1}$  (see ref. [6]). With both geometries (2D without TJs or 3D with TJs), lattice diffusion is found to be the same and to be faster in nano-grains than in mono-Si. In nano-grains  $D_g = 1.97 \times 10^{-4} \exp(-2.92 \text{ eV}/kT) \text{ cm}^2 \text{ s}^{-1}$ . However, GB diffusion is found to be different using either the 2D geometry or the 3D geometry. Without considering TJs, GB diffusion is found to be 10 times faster in nano-GB compared to micro-GBs. Though, even considering constant TJ diffusion over the entire annealing temperature range, GB diffusion is found to be similar in nano-GBs and micro-GBs, as already suggested in other experiments [11].

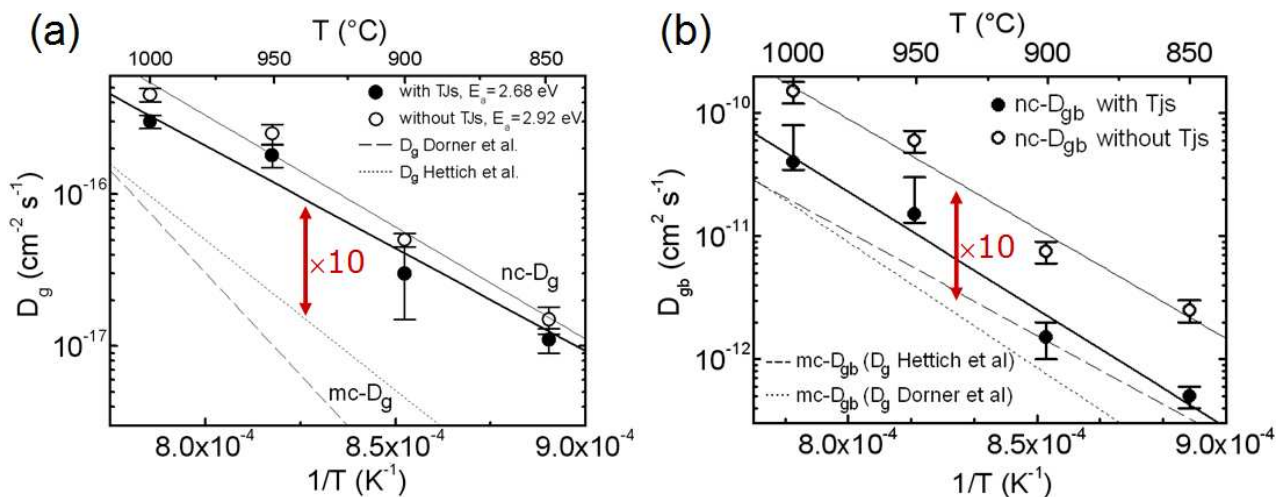


Fig. 3. Ge diffusion coefficients measured in nc-Si using a model without TJs (open circles) or a model with a constant diffusion coefficient in TJs (solid circles): (a) comparison between lattice diffusion in monocrystalline Si (broken lines) and in 40 nm-wide grains, (b) comparison between GB diffusion in mc-Si (from fig. 2, broken lines) and nc-Si.

Considering that  $D_{gb}$  is the same in mc-Si and nc-Si, the Ge TJ diffusion coefficient was measured using 3D FES [6]. We found  $D_{Tj} = 5.72 \times 10^4 \exp(-3.24 \text{ eV}/kT) \text{ cm}^2 \text{ s}^{-1}$ , with  $D_{Tj} \sim 4.7 \times 10^2 D_{gb}$ . Consequently, TJ diffusion in nc-Si is not negligible even for 40 nm-wide grains, and the fast diffusion observed in nc-Si compared to mc-Si results from faster diffusion in nano-grains and fast diffusion in TJs.

### Nano-size effect upon reactive diffusion

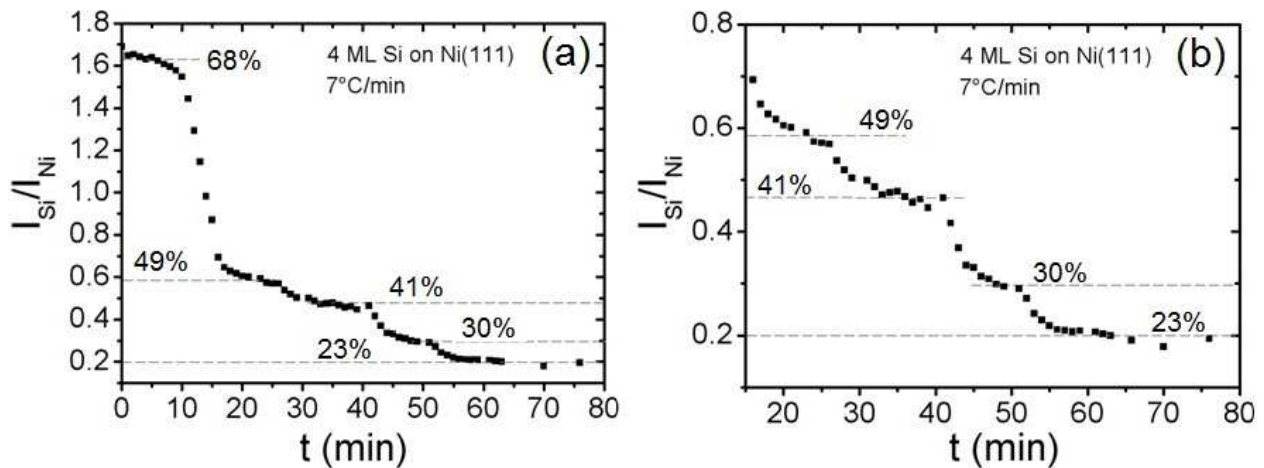


Fig. 4. AES signal recorded in situ during the reaction of 4 Si MLs on Ni(111), annealing ramp of  $7^{\circ}\text{Cmin}^{-1}$ . Corresponding Si content calculated from the AES signal is also shown.

Fig. 4 presents the ratio between Si and Ni Auger electron spectroscopy (AES) signals acquired in situ during the reaction of a 5 monolayer (ML)-thick Si film on a Ni(111) substrate, during an annealing ramp of  $7^{\circ}\text{C min}^{-1}$  [8]. We observe 5 pseudo-plateaus and several breaks in the reaction kinetic, which seems to correspond to the sequential formation of the 6 compounds in the Ni-Si phase diagram in this temperature range, from the Si-rich to the Ni-rich compounds, if we calculate from the AES signal at plateaus the concentration of a uniform Ni-Si solid solution ( $\text{NiSi}_2$ [67%],  $\text{NiSi}$ [50%],  $\text{Ni}_3\text{Si}_2$ [40%],  $\text{Ni}_2\text{Si}$ [33%],  $\text{Ni}_3\text{Si}_{12}$ [28%],  $\text{Ni}_3\text{Si}$ [25%]) [8]. Similarly to experiments, atomistic KMC simulations of the reaction of a thin film made of A atoms on a face centered cubic (fcc) substrate made of B atoms (A-B binary system with ordering tendency) show that phase growth follows two regimes [7].

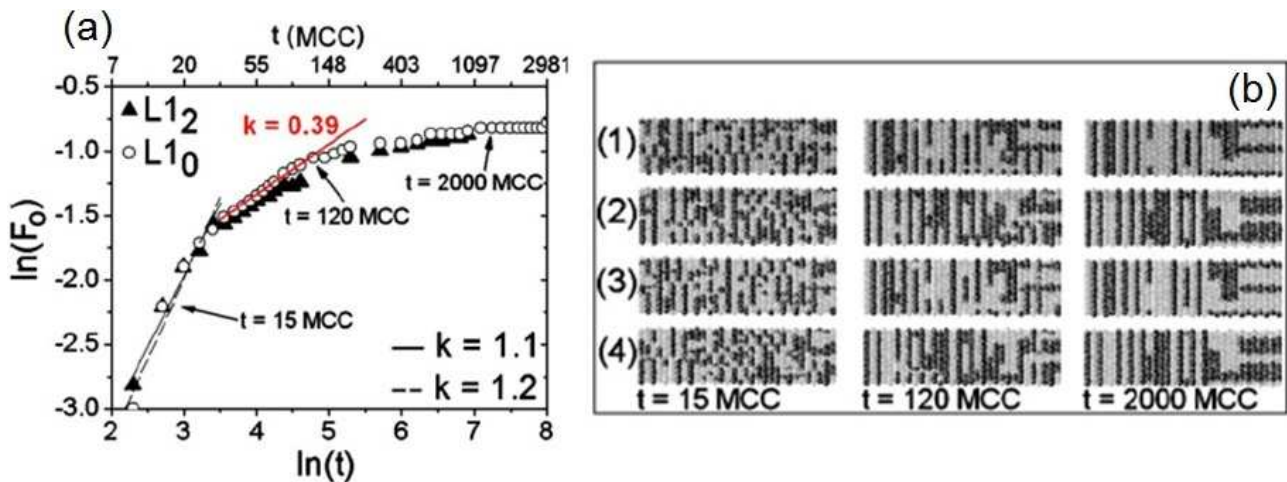


Fig. 5. Atomistic KMC simulations of the formation of a phase ( $L_{12}$  and  $L_{10}$  on fcc lattice) in the bulk of a random binary solution with an average concentration corresponding to the phase stoichiometry: (a) time variations of the volume fraction ( $F_0$ ) of the phase, and (b) four consecutive atomic planes in the bulk of the sample at the three different times corresponding to the three arrows in (a) for the  $L_{10}$  phase.

First, the phase volume increases linearly with time, and second, it increases as the time root mean square (linear-parabolic transition). However, similar simulations show that phase formation in bulk follows the same trend. Fig. 5a presents the time variation of the phase ( $L_{12}$  and  $L_{10}$  on fcc lattice) volume fraction  $F_0$  in the sample bulk during phase formation from random solid solution. Fig. 5b presents the atomic distribution of 4 consecutive (001) planes in the sample bulk at 3 different times corresponding to the  $L_{10}$  phase growth in the linear (15 Monte Carlo cycles) and the parabolic régimes (120 MCC), as well as in the last regime with ordered domain stabilization (2000 MCC).

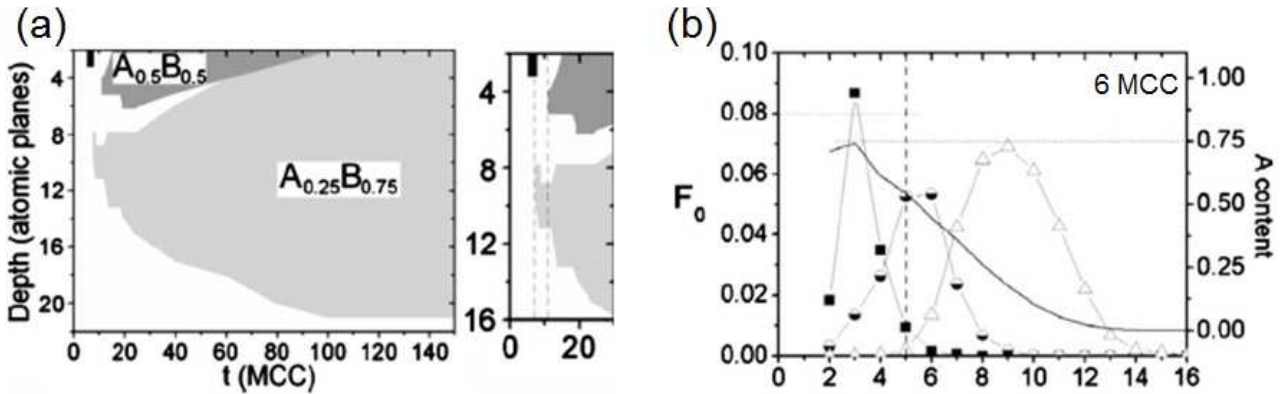


Fig. 6. Atomistic KMC simulations of the reaction of a 5 ML-thick film on a fcc substrate for a symmetric system composed of A and B atoms, and exhibiting three bulk phases ( $A_{0.75}B_{0.25}$ ,  $A_{0.5}B_{0.5}$  and  $A_{0.25}B_{0.75}$ ): (a) phase location in the bulk of the sample (plan #1 is the surface) versus time, and (b) comparison between the phase fraction of each of the three phases (left axis,  $A_{0.75}B_{0.25}$ —solid squares,  $A_{0.5}B_{0.5}$ —semi-solid circles and  $A_{0.25}B_{0.75}$ —open triangles) and composition (right axis, A at.%) versus depth.

The linear regime corresponds to the beginning of phase formation without long range atom transport, and the parabolic regime corresponds to the improvement of ordering domains thanks to atom diffusion. The linear-parabolic transition observed during the reaction of a nano-film on a substrate is not related to an interface effect nor to a diffusion asymmetry, since in our simulations the diffusivity of A in B is the same as B in A. In the case of film reaction, the linear regime corresponds to phase nucleation, and the parabolic regime corresponds to phase growth supported by atomic diffusion in the phases present in the bulk [7]. Similarly to experiments, atomistic KMC simulations show that phase formation exhibits a simultaneous-sequential transition versus film thickness [7]. For thick films the phases appear simultaneously. However, in case of thin films, phases can appear sequentially, only two phases coexisting in the bulk: the new growing phase and the old consumed phase. Fig. 6a presents phase formation during the reaction of a 5 ML-thick A film on a B substrate: the phases ( $A_{0.75}B_{0.25}$ ,  $A_{0.5}B_{0.5}$ ,  $A_{0.25}B_{0.75}$ ) appear sequentially starting with the film-atom richest phase. Fig. 6b shows the 3 ordered fractions of the 3 phases (left axis) and the composition ( $C_A$ , right axis) versus depth (atomic planes) when the first phase appears (6 MCC), i.e.  $F_0 \geq 0.08$  [7].

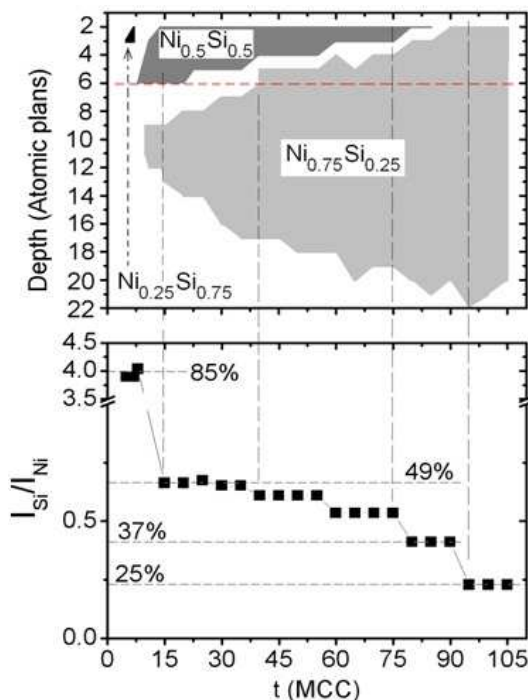


Fig. 7. Simulated AES signal using atomistic KMC simulation results corresponding to the reaction of a 5 ML-thick pseudo-Si film on a Ni substrate.

Due to the finite size of the film and the semi-infinite size of the substrate, an asymmetric interdiffusion profile has formed between A and B. In the film  $C_A \sim 0.75$  triggering the formation of  $A_{0.75}B_{0.25}$  ( $F_0 \geq 0.08$ ), while in the substrate the diffusion profile does not yet allow the formation of the other phases ( $F_0 < 0.08$ ). The nano-size effect on phase formation is thus related to the formation of an asymmetric interdiffusion profile in the film and the substrate promoting sequential phase formation [7]. Considering Ni-Si compound formation energies, one can define an averaged Ni-Si pair interaction [8] and simulate the reaction of a 5 ML-thick pseudo-Si film on a Ni substrate by KMC. Fig. 7 presents the results of the KMC simulations and the corresponding AES signal. These results are in qualitative agreement with the experimental AES measurements presented in fig. 4. The Ni-Si phases appear sequentially from the Si-rich to the Ni-rich phases during the reaction of a sub-nanometric Si film on Ni.

### Summary

We presented experimental and theoretical results concerning nano-size effects upon atomic diffusion and ultra-thin film reaction related to materials involved in the microelectronic Si technology. Ge diffusion in Si nano-crystals appears to be faster than in mono-Si, however, Ge diffusion in nano-GBs is found to be similar as in micro-GBs. Ge TJ diffusion is not negligible in nc-Si exhibiting 40 nm-wide grains. TJ diffusion is found to be about 3 orders of magnitude faster than GB diffusion. Comparison between experiments and atomistic simulations shows that sub-nanometric film reaction exhibits sequential phase formation from the film-atom rich phases to the substrate-atom rich phases. Sequential phase formation results from an asymmetric interdiffusion profile between the film and the substrate due to the finite size of the film compared to the infinite size of the substrate, even without diffusion asymmetry.

### References

- [1] I.-S. Kang, Y.-S. Kim, H.-S. Seo, S.W. Son, E. A. Yoon, S.-K. Joo, and C.W. Ahn: *Appl. Phys. Lett.* Vol. 98 (2011), p. 212102
- [2] T. Wang and P. Peumans: *J. Appl. Phys.* Vol. 109 (2011), p. 114301
- [3] A. Portavoce, M. Kammler, R. Hull, M.C. Reuter and F.M. Ross: *Nanotechnology* Vol. 17 (2006), p. 4451
- [4] K. Houmada, A. Portavoce, C. Perrin-Pellegrino, D. Mangelinck, and C. Bergman: *Appl. Phys. Lett.* Vol. 92 (2008), p. 133109
- [5] A. Portavoce, G. Chai, L. Chow, and J. Bernardini: *J. Appl. Phys.* Vol. 104 (2008), p. 104910
- [6] A. Portavoce, L. Chow, and J. Bernardini: *Appl. Phys. Lett.* Vol. 96 (2010), p. 214102
- [7] A. Portavoce and G. Tréglia: *Phys. Rev. B* Vol. 82 (2010), p. 205431
- [8] A. Portavoce, B. Lalmi, G. Tréglia, C. Girardeaux, D. Mangelinck, B. Aufray, and J. Bernardini: *Appl. Phys. Lett.* Vol. 95 (2009), p. 023111
- [9] G. Hettich, H. Mehrer, and K. Maier: *Inst. Phys. Conf. Ser.* Vol. 46 (1979), p. 500
- [10] P. Dorner, W. Gust, B. Predel, U. Roll, A. Lodding, and H. Odelius: *Philos. Mag. A* Vol. 49 (1984), p. 557
- [11] Z. Balogh, Z. Erdélyi, D.L. Beke, A. Portavoce, C. Girardeaux, J. Bernardini, A. Rolland: *Appl. Surf. Sci.* Vol. 255 (2009), p. 4844

**Diffusion in Materials - DIMAT 2011**  
10.4028/www.scientific.net/DDF.323-325

**Nanometric-Size Effect upon Diffusion and Reaction in Semiconductors:  
Experimental and Theoretical Investigations**  
10.4028/www.scientific.net/DDF.323-325.433